Journal of Thermal Analysis and Calorimetry (2022) 147:10383–10390
https://doi.org/10.1007/s10973-022-11277-9

Tunable flammability studies of graphene quantum dots-based polystyrene nanocomposites using microscale combustion calorimeter

Rong Ma[1] · Ruiqing Shen[1] · Yufeng Quan[1] · Qingsheng Wang[1]

Received: 6 September 2021 / Accepted: 12 February 2022 / Published online: 10 March 2022

Abstract
Polymer composites with improved thermal and flame-retardant performance are imperative for fire-safe materials. Carbon-based nanomaterials have the advantages of low cytotoxicity, chemical inertness, cost-effectiveness, and biocompatibility. Graphene quantum dots (GQDs) as a new member of carbon-based nanomaterials were fabricated by pyrolysis method, and easy to be functionalized to fabricate nanocomposites as efficient flame retardant. Herein, polystyrene (PS) nanocomposites with introduction of modified graphene quantum dots (C-GQDs) were fabricated by the Pickering emulsion polymerization method. The C-GQDs with controllable chemical structure could be used as stabilizer in emulsion polymerization system and introduced to PS directly. Morphological and chemical characterization of PS nanocomposites revealed that the successful introduction of C-GQDs to PS, and C-GQDs were wrapped on the surface of PS microspheres. The flammability behavior of the PS nanocomposites was investigated by using microscale combustion calorimeters (MCC), and the peak heat release rate of PS nanocomposite was reduced 40% when compared with that of neat PS. The improved flame retardancy was mainly attributed to the C-GQDs promoting the formation of physical protective barrier on the surface, which impeded the permeation of heat and the pyrolysis products. Therefore, a facile method for preparing nanocomposite has been developed in this work, and C-GQDs could be used as flame retardants to reduce the flammability of polystyrene nanocomposites system.

Keywords Polystyrene · Graphene quantum dots · Emulsion polymerization · Microscale combustion calorimeters · Flammability

Introduction

Polymer materials have been widely used in industry and daily life. Polystyrene (PS) is a kind of thermoplastic polymer with wide-spread application due to its outstanding properties including low density, excellent mechanical durability, and good processing capabilities [1]. However, the production of a large number of combustible volatiles and smoke during the combustion process, which would lead to injuries and death in a fire, will limit its further application [2–5]. Therefore, it is necessary to improve the flame retardancy. Due to safety and environmental protection requirements, halogen-free flame retardants have attracted great attention [6, 7]. According to published work, nanomaterials showed great potential to improve flame retardancy. Nanoclay [8–10], molybdenum disulfide [11], zirconium phosphate [12], layered doubled hydroxides [13–15], silica nanoparticles [16], etc., all presented that the fabricated nanocomposites exhibited improved fire retardance.

The rise of carbon-based materials has attracted considerable interest for fabricating composites with improved performance, such as mechanical, gas barrier, and flame-retardant properties [17, 18]. Carbon-based nanomaterials, such as graphene and carbon nanotubes (CNTs), have presented high flame-retardant efficiency in polymer composites. Recent work shows that the PS incorporated with porous carbon sheet would benefit to remarkably reduce flammability [19]. Graphene showed stability against combustion, so it has been used directly to prepare flame-retardant polymer composites. Previous work found that the peak heat release rate (pHRR) was decreased to 50% compared with that of neat PS when the incorporation content of graphene was 5 mass%

✉ Qingsheng Wang
qwang@tamu.edu

[1] Artie McFerrin Department of Chemical Engineering, Texas A&M University, College Station, TX 77843, USA

[20]. However, the pristine carbon-based nanomaterials have the incompatibility problem which would lead to inferior behavior [17]. The surface modification method has been applied for carbon-based nanomaterials to overcome this obstacle. Applied graphene sheets decorated with titanium dioxide nanoparticles into polymer, polymer nanocomposite exhibited reduced pHRR values and suppressed emission of carbon dioxide [21]. Xing et al. [22] fabricated PS nanocomposites with modified CNTs which functionalized with phosphorus- and nitrogen-containing agents. The fabricated PS nanocomposites presented improved thermal stability and tensile strength due to good dispersion and interfacial interaction between modified CNTs and PS matrix.

Graphene quantum dots (GQDs) are a kind of 0-dimensional nanomaterials. Compared with graphene sheets, GQDs are more feasible to be functionalized due to the prevalence of chemical active groups at the edge, and have smaller size and high specific area, which are benefit to fabricate nanocomposite. Additionally, GQDs have shown the potential to enhance the flame retardancy. Khose et al. [23] coated functionalized GQDs with phosphorous agent on cotton cloth, which does not change the color and improved the flame retardancy of cotton cloth. Rahimi-Aghdam et al. [24] synthesized nitrogen and phosphorous co-doped graphene quantum dots (NP-GQDs) and introduced them into polyacrylonitrile (PAN) by solvent blending route. The fabricated PAN nanocomposites showed improved flame retardancy. The pHRR of PAN nanocomposites decreased by 15.4% compared with bare PAN. However, the solvent blending method would consume a great number of toxic organic solvents, such as chloroform. Therefore, applying GQDs to prepare polymer nanocomposites with a facile and environmentally friendly method to improve flame retardancy remains challenge.

Herein, we fabricated PS nanocomposites which were incorporated with modified GQDs (C-GQDs) via a simple one-pot method. The C-GQDs were synthesized based on our previous work [25]. The C-GQDs have controllable amphiphilicity could be used to stabilize oil-in-water emulsion and have potential to be used directly for Pickering emulsion polymerization without surfactant. The various reports have showed that the Pickering emulsion polymerization is a fascinating and feasible method to fabricate novel polymer nanocomposites, and it would consume small amount of organic solvent than solution mixing method [26, 27]. The aim of this work is to reduce the fire hazards of PS by introducing C-GQDs onto the surface of the PS microsphere. The flammability of PS nanocomposites system is evaluated by using a microscale combustion calorimeter (MCC) due to the accuracy of the measured results independent on experimental conditions and external physical factors [28], and the mechanism of reduced fire hazards of PS is also discussed.

Experimental

Materials

Styrene (≥ 99%), sodium dodecyl sulfate (SDS, ≥ 99.0%), and initiator azobis (isobutyronitrile) (AIBN, 98%) were purchased from Sigma. The amphiphilic graphene quantum dots (C-GQDs) were synthesized based on our previous work [25]. In brief, the C-GQDs was pyrolyzed by citric acid and dodecylamine at 200 °C in air. All purchased chemicals were used as received without purification.

Fabrication of PS/C-GQDs nanocomposites

The PS/C-GQDs nanocomposites were fabricated by Pickering emulsion polymerization which used C-GQDs as a stabilizer. The emulsion polymerization process illustration is shown in Fig. 1a. The C-GQDs were dispersed in deionized (DI) water with different concentrations as aqueous phase. The oil phase contained styrene and 2.0 mass% AIBN. The aqueous phase and oil phase were added into a vial and sonicated (frequency ~ 20 kHz) for 1 min to form a stable Pickering emulsion. Afterwards, this mixture was heated at 80 °C for 6 h. Finally, the products were washed with DI water three times and then dried by freeze dryer. The obtained PS/C-GQDs nanocomposites were named as PS/C-GQD 1, PS/C-GQD 2, PS/C-GQD 3, PS/C-GQD 4, and PS/C-GQD 5, respectively, according to the C-GQDs concentration in aqueous solution of 0.1%, 0.5%, 1.0%, 1.5%, and 2.0%. For comparison, the PS emulsion polymerization was carried out with the same conditions except that the C-GQDs was replaced by 0.1% SDS in aqueous phase.

Characterization

The chemical structure and composition were investigated by Fourier transform infrared spectroscopy (FTIR, Thermo Nicolet 380) and Omicron's DAR X-ray photoelectron spectroscopy (XPS, excitation source: Mg Kα radiation). The morphologies of PS/C-GQDs nanocomposites were investigated by a field emission scanning electron microscope (FE-SEM, JEOL JSM-7500F, Japan). The thermal stability was investigated by thermogravimetric analysis (TGA) using TGA device (TA Instrument Q500). This was conducted from 30 to 750 °C with 20 °C min^{-1} heating rate under N_2 atmosphere. A microscale combustion calorimeter (MCC, Fire Testing Technology, United Kingdom) was used to evaluate the combustion properties. The presented results of each sample were tested at least three times and the average values were calculated.

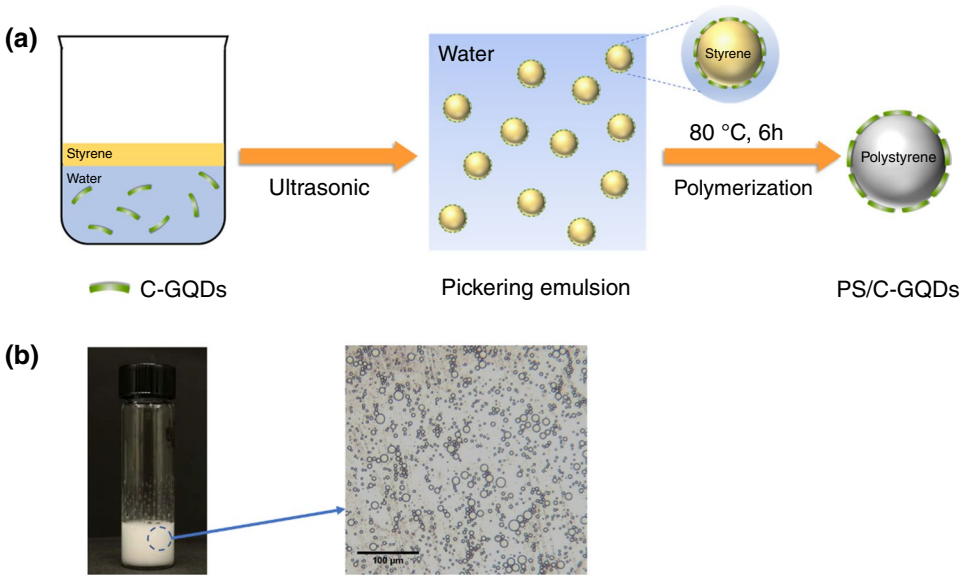

Fig. 1 **a** Schematic illustration of the synthetic process to prepare PS/C-GQDs nanocomposites. **b** Styrene-in-water emulsion stabilized by 0.1 mass% C-GQDs

Results and discussion

Chemical structure and morphology of nanocomposites

Based on our previous work [25], the synthesized C-GQDs had amphiphilic properties which could be used to stabilize oil-in-water emulsions. Meanwhile, the nanoparticle would be location-selective via an oil-in-water emulsion system [29]. The nanocomposite covered with nanoparticles on the surface could be prepared by dispersing the nanoparticles in the aqueous phase [29]. Here, we used the amphiphilic C-GQDs to stabilize styrene-in-water emulsion by sonication. As shown in Fig. 1b, this is capable of forming stable styrene-in-water emulsions. Then, the PS/C-GQDs nanocomposites were fabricated through Pickering emulsion polymerization with C-GQDs in aqueous phase as a stabilizer. FTIR and XPS spectra were employed to investigate the chemical structure and composition of PS/C-GQDs nanocomposites as shown in Fig. 2. The FTIR spectroscopy (Fig. 2a) was employed to detect the modified materials. The peaks at 3025 cm^{-1} are ascribed to the C–H stretching vibration of the aromatic ring [26]. The peaks at 1492 and 1452 cm^{-1} are corresponding to the C–C stretching of the benzene ring [26]. These results indicate that PS has been synthesized successfully. Compared to neat PS, there are some other strong peaks observed in PS/C-GQDs nanocomposites which are typical peaks of C-GQDs. The absorption bands

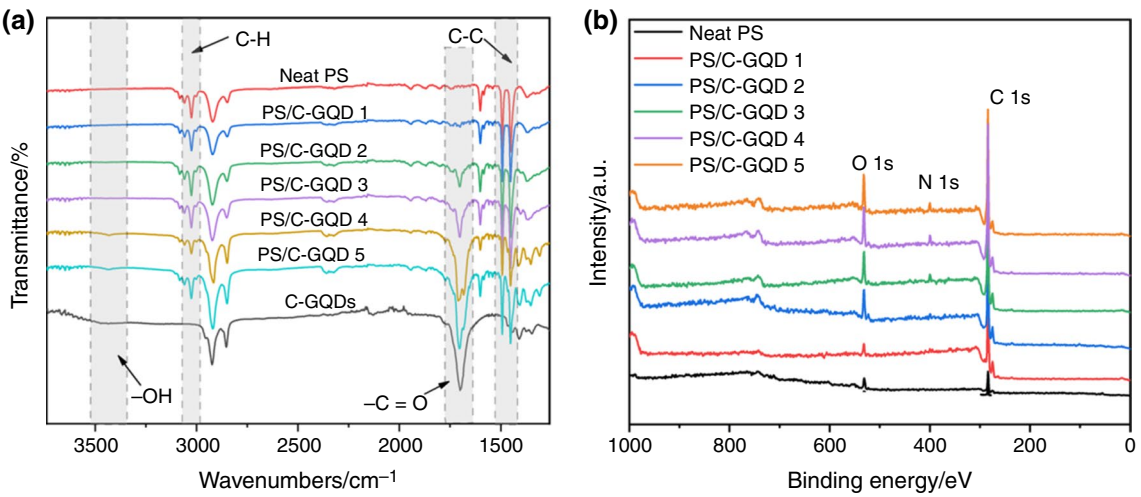

Fig. 2 **a** FTIR and **b** XPS spectra of neat PS and PS/C-GQDs nanocomposites

at 1690 and 3459 cm^{-1} are attributed to an amide group and –OH group, respectively [25], which are verified by the spectrum of C-GQDs. Correspondingly, the intensity of these two peaks becomes stronger with the increasing C-GQDs concentration in aqueous phase. Therefore, it is evidence of the direct incorporation of C-GQDs into the PS nanocomposites via Pickering emulsion polymerization. In addition, the chemical composition of resulting nanocomposites was investigated by XPS as shown in Fig. 2b. When increasing the C-GQDs concentration from 0 to 2 mass%, the nitrogen concentration increases from 0 to 3.6 mol% on the PS microspheres' surface. These results confirm that the C-GQDs have been introduced to PS/C-GQDs nanocomposites successfully.

The surface morphologies of neat PS and PS/C-GQDs nanocomposites were characterized by FE-SEM. As shown in Fig. 3, the products are all microsphere structures and the surface of neat PS microspheres is smooth. The morphology of C-GQDs was investigated by TEM as shown in Fig. S1. After incorporation of C-GQDs on the surface, the surface of the PS/C-GQDs nanocomposites becomes rough. For PS/C-GQD 5 samples, there are clearly wrinkled C-GQDs assembled on the microsphere surface. These results also indicate that the C-GQDs have been introduced on the surface of PS microspheres.

Thermal stability assessment of nanocomposite

The TGA was conducted to investigate the thermal degradation behavior of as-prepared samples. Figure 4a presents the TGA curves of neat PS and modified systems. The relevant thermal property data are summarized in Table 1. Under nitrogen conditions, the pure PS exhibits the only one-stage decomposition process, occurring in the range of 350–450 °C, which is attributed to a chain-scissoring process. However, the three-stage decomposition behavior is observed for the modified systems. For PS/C-GQD 4 and PS/C-GQD 5 nanocomposites, the decomposition stage in the range of 380–470 °C is similar to that in the neat PS. The first and third step decomposition ranging from 280–380 to 520–600 °C is initiated by C-GQDs, which is similar to the decomposition stage of C-GQDs. The first stage of mass loss is

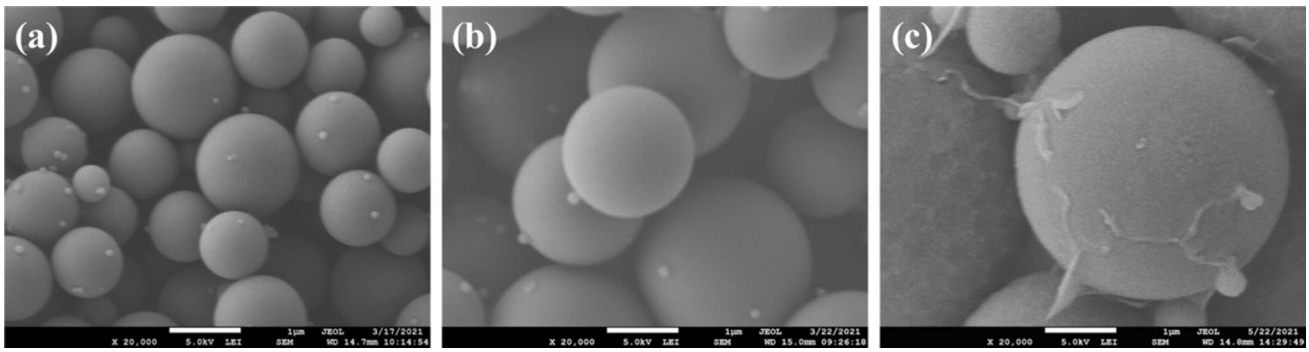

Fig. 3 Surface SEM morphologies for **a** neat PS, **b** PS/C-GQD 1 and **c** PS/C-GQD 5, respectively

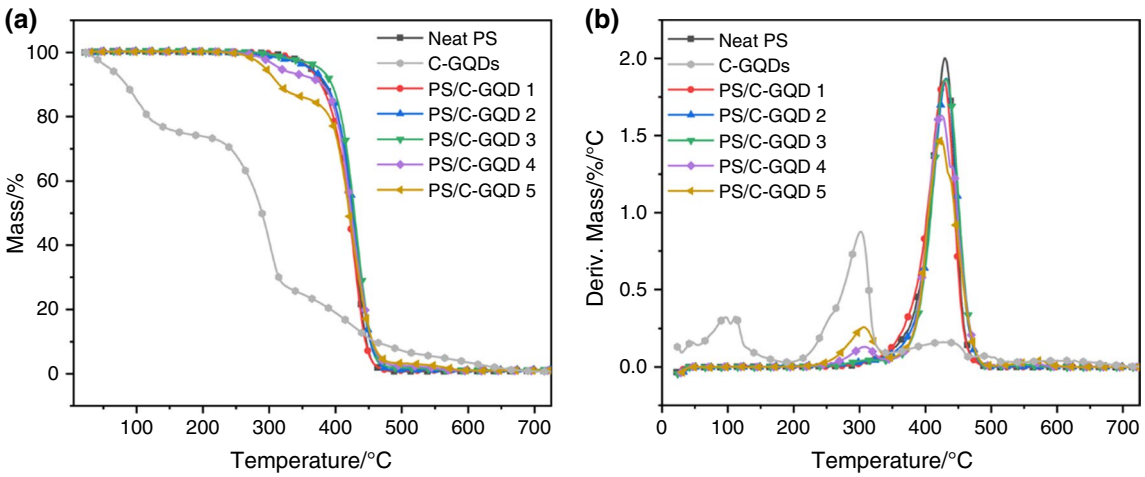

Fig. 4 **a** TGA and **b** DTG curves of PS and PS/C-GQDs nanocomposites

Table 1 TGA data of PS and PS/C-GQDs nanocomposites

Sample no.	$T_{-10\%}$ /°C	$T_{-50\%}$ /°C	T_{max} /°C	T_{in} /°C	Residue at 700 °C (%)	
					Exp	Cal
Neat PS	383	423	429	287	0.77	0.77
PS/C-GQD 1	378	420	428	290	1.07	0.86
PS/C-GQD 2	385	426	431	321	1.15	0.86
PS/C-GQD 3	394	428	431	348	1.26	0.85
PS/C-GQD 4	379	423	424	354	1.00	0.84
PS/C-GQD 5	314	420	423	358	1.05	0.84

T_{in} the initial decomposition temperature of main mass loss

attributed to the removal of functional groups on C-GQDs [30]. After introducing C-GQDs, the onset degradation temperature at 10 mass% mass loss ($T_{-10\%}$) and the temperature at 50% mass loss ($T_{-50\%}$) are increased significantly. The maximum increase of $T_{-10\%}$ and $T_{-50\%}$ is 13 and 5 °C, respectively, indicating that the thermal stability of the PS host is significantly improved. Nevertheless, the $T_{-10\%}$ values of PS/C-GQD 5 nanocomposites with high C-GQDs content are lower than that of neat PS, which might be explained as the cleavage of functional group on C-GQDs such as −OH and amide groups. Although the onset degradation temperature of PS/C-GQD 5 is lower, the maximum mass loss rate decreased significantly as shown in Fig. 4b. From DTG curve, the rate of mass loss of PS/C-GQDs decreases with increasing C-GQDs content in nanocomposites compared with neat PS. The maximum mass loss rate for PS/C-GQD 5 is reduced by 27% relative to that of neat PS, although the temperature of maximum degradation rate (T_{max}) does not change significantly. Meanwhile, the initial decomposition temperature of main mass loss (T_{in}) is delayed remarkably as shown in Table 1, which indicates that the pyrolysis process of PS/C-GQDs nanocomposites is retarded. In addition, it is noteworthy that the residual yield of PS/C-GQD 5 is 1.6 times that of neat PS at temperature 700 °C.

To further understand the effect of C-GQDs on the thermal stability of PS nanocomposites, it is assumed that the calculated value of the residual yield (Y^{Cal}) of PS nanocomposites follow the linear mixing rule, as seen in Eq. (1) [6, 31]:

$$Y^{Cal} = Y_{PS} \times f_{w,\,PS} + Y_{C\text{-}GQDs} \times f_{w,\,C\text{-}GQDs} \quad (1)$$

where Y_{PS} and $Y_{C\text{-}GQDs}$ represent the residual yield of neat PS and C-GQDs, respectively, and $f_{w,\,PS}$ and $f_{w,\,C\text{-}GQDs}$ refer to the mass fraction of neat PS and C-GQDs, respectively.

According to the calculated results presented in Table 1, the Y^{Cal} values of PS nanocomposites are much lower than that of the corresponding experimental values. The residue of PS nanocomposite at 700 °C was higher than the calculated values. Specially, the PS/C-GQD 3 shows an increase of Y^{Cal} value by a factor of 148% under experimental conditions, which indicates that the decomposition of PS chain is inhibited by the incorporation of C-GQDs. These results imply that the decomposition of PS at a high temperature was inhibited under a nitrogen atmosphere. It suggests that the incorporation of C-GQDs promotes the residue layer formation to create a protective layer on the surface during the decomposition process. The physical barriers could retard the mass transfer from condensed phase towards the flame gas phase and inhibit heat transfer from heat source to condensed phase. Therefore, the thermostability of PS/C-GQDs nanocomposites is improved.

Flammability behavior of nanocomposites

MCC was widely used to evaluate flammability behavior of polymeric materials. The samples were heated during the MCC evaluation process, and the heat of combustion of pyrolysis products was measured directly. The pHRR, THR, and heat release capacity (HRC) of PS and PS/C-GQDs were primary parameters obtained by MCC, and the

Table 2 Summaries of MCC data for PS and PS/C-GQDs nanocomposites

Sample no	pHRR /W g^{-1}	HRC /J g^{-1} K^{-1}	THR / kJ g^{-1}	T_{pHRR} /°C	Reduct-HRC[a]/%
Neat PS	868	889	37.0	443	NA
PS/C-GQD 1	771	787	36.0	443	11
PS/C-GQD 2	653	670	33.5	442	24
PS/C-GQD 3	612	627	34.1	442	29
PS/C-GQD 4	554	564	32.6	444	36
PS/C-GQD 5	520	527	35.3	441	40

[a]Reduct-HRC, $100 \times (HRC_{polymer} - HRC_{nanocomposite})/HRC_{polymer}$

corresponding data are given in Table 2. For PS modified by C-GQDs, there is a dramatic decrease of the pHRR values with increasing C-GQDs content in aqueous phase (Fig. 5a). The pHRR value decreases from 868 W g^{-1} of neat PS to 520 W g^{-1} of PS/C-GQD 5, which indicates that the flame retardancy of PS nanocomposites has been improved significantly. The THR values are also reduced by introducing C-GQDs, which indicates that the PS/C-GQDs nanocomposite not all the polymer burns. Under normal MCC operation conditions, the combustion of gas products occurs in excess of oxygen, so it is typically a complete combustion [32]. The 40% reduction of pHRR values suggests that there are fewer volatile products transferring to gas phase. For PS/C-GQD 5 nanocomposites, there is an obvious peak before the main PS pyrolysis peak, which is similar to the decomposition peak of C-GQDs. It coincides with the TGA behavior, in which there is a thermal decomposition of C-GQDs at a lower temperature than main decomposition stage. This phenomenon suggests that the C-GQDs would initially be decomposed to form a barrier layer to inhibit the permeation of heat and volatile products.

HRC could be used as a good predictor of flammability, which was independent of the form and mass of samples as long as the temperature of sample is uniform during the test [28, 33, 34]. A tendency of nanocomposite system in HRC has been found that the C-GQDs is a good candidate for reducing HRC, which indicates lower flammability resulting in a lower risk of fire hazard [30]. The comparison of the reduction in HRC (Reduct-HRC) suggests that introducing more C-GQDs on PS sphere is benefit to improve flame retardancy. Therefore, the improved flame retardancy is attributed to the presence of C-GQDs on the surface, and rendering excellent flame retardancy for the PS nanocomposite system based on the barrier effect.

Based on the results above, the improved thermal stability and flame retardancy are attributed to the fact that the C-GQDs assembled at the surface of PS microsphere. The proposed mechanisms for the improved flame-retardant performance of PS nanocomposites are illustrated in Fig. 5c. For neat PS, amount of volatile gas emerged due to rapid decomposition of neat PS. When C-GQDs were introduced on the PS microsphere surface, the graphite carbon in C-GQDs could benefit to improve the quality of protective layer. It would retard the transfer of heat and pyrolysis gas products. The barrier effect by protective layer becomes more prominent with increasing C-GQDs content on surface.

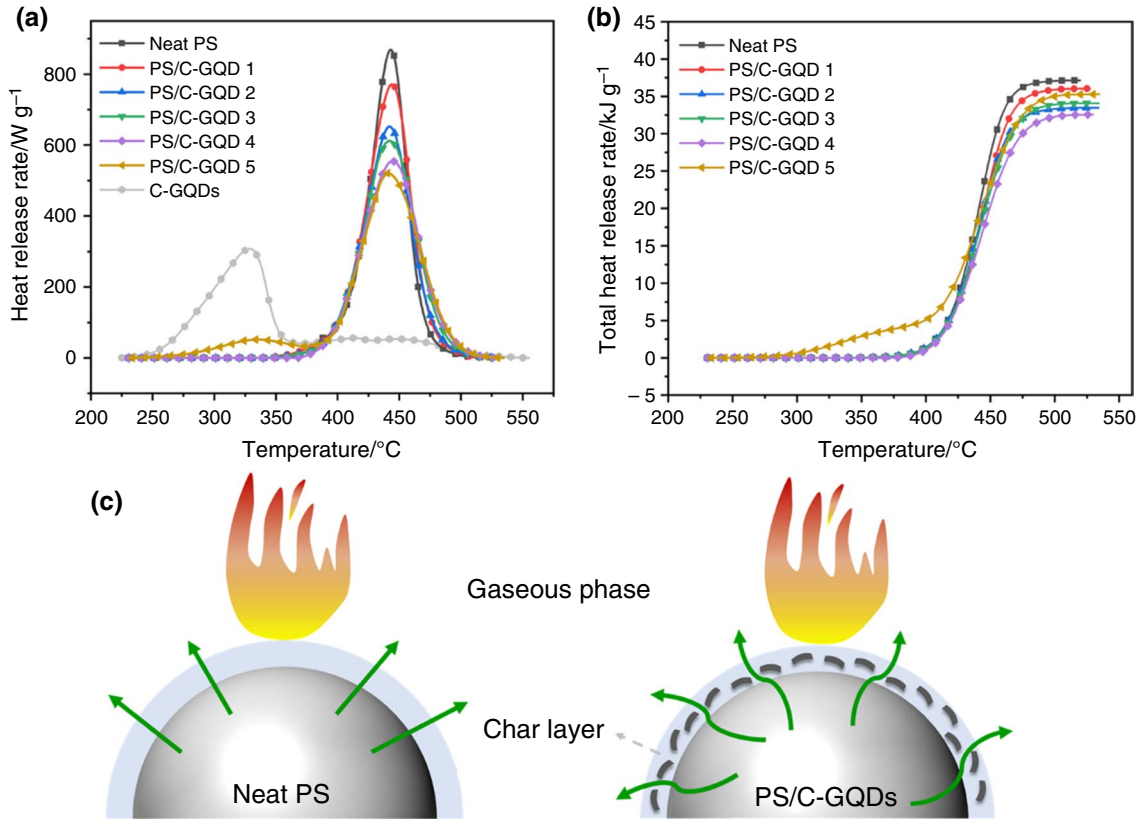

Fig. 5 **a** HRR and **b** THR curves of PS and PS/C-GQDs nanocomposites. **c** Proposed mechanisms of flame retardancy of PS nanocomposites

Conclusions

In this work, a PS nanocomposite system with C-GQDs as flame retardant was fabricated by Pickering emulsion polymerization, which applied C-GQDs as stabilizers in the polymerization process. Morphological characterization revealed that the C-GQDs were coated onto the PS microsphere surface via this polymerization method. The incorporation of C-GQDs onto the PS surface increased the thermal stability of PS nanocomposites, including a maximum increase of 13 °C in $T_{-10\%}$ and the maximum mass loss rate is reduced by 27% relative to that of neat PS. Moreover, the value of pHRR for PS/C-GQD 5 decreased by around 40%, which exhibits similar or more reduction in pHRR values when compared with other PS nanocomposites incorporated with graphene sheets (as shown in Table S1). These significant improvements in PS nanocomposites were attributed to the stronger residue barrier layer which was provided by C-GQDs. Thus, this work would provide a potential effective method that broadens the application of polymer nanocomposites into excellent flame retardancy.

Supplementary Information The online version contains supplementary material available at https://doi.org/10.1007/s10973-022-11277-9.

Acknowledgements The authors acknowledge the use of the Materials Characterization Facility (MCF) at Texas A&M University for SEM. The authors also thank Dr. Hung-Jue Sue for using TGA instrument.

Declarations

Conflict of interest The authors declare that they have no conflict of interest.

References

1. Wang Y, Meng X, Wang C, Han Z, Shi H. Fire reaction properties of polystyrene-based composites using hollow silica as synergistic agent. J Therm Anal Calorim. 2020;8:1–8.
2. Chen X, Jiang Y, Jiao C. Smoke suppression properties of ferrite yellow on flame retardant thermoplastic polyurethane based on ammonium polyphosphate. J Hazard Mater. 2014;266:114–21.
3. Zhou K, Wang B, Jiang S, Yuan H, Song L, Hu Y. Facile preparation of nickel phosphide ($Ni_{12}P_5$) and synergistic effect with intumescent flame retardants in ethylene–vinyl acetate copolymer. Ind Eng Chem Res. 2013;52:6303–10.
4. Chen X, Wei S, Gunesoglu C, Zhu J, Southworth CS, Sun L, Karki AB, Young DP, Guo Z. Electrospun magnetic fibrillar polystyrene nanocomposites reinforced with nickel nanoparticles. Macromol Chem Phys. 2010;211:1775–83.
5. Brannum DJ, Price EJ, Villamil D, Kozawa S, Brannum M, Berry C, Semco R, Wnek GE. Flame-retardant polyurethane foams: one-pot, bioinspired silica nanoparticle coating. ACS Appl Polym Mater. 2019;1:2015–22.
6. Wang Z, Liu Y, Li J. Regulating effects of nitrogenous bases on the char structure and flame retardancy of polypropylene/intumescent flame retardant composites. ACS Sustain Chem Eng. 2017;5:2375–83.
7. Chen MJ, Lazar S, Kolibaba TJ, Shen R, Quan Y, Wang Q, Chiang H-C, Palen B, Grunlan JC. Environmentally benign and self-extinguishing multilayer nanocoating for protection of flammable foam. ACS Appl Mater Interfaces. 2020;12:49130–7.
8. Li Z, Liu L, Jiménez González A, Wang DY. Bioinspired polydopamine-induced assembly of ultrafine $Fe(OH)_3$ nanoparticles on halloysite toward highly efficient fire retardancy of epoxy resin via an action of interfacial catalysis. Polym Chem. 2017;8:3926–36.
9. Ahmed L, Zhang B, Shen R, Agnew RJ, Park H, Cheng Z, Mannan MS, Wang Q. Fire reaction properties of polystyrene-based nanocomposites using nanosilica and nanoclay as additives in cone calorimeter test. J Therm Anal Calorim. 2018;132:1853–65.
10. Qin P, Yi D, Xing J, Zhou M, Hao J. Study on flame retardancy of ammonium polyphosphate/montmorillonite nanocompound coated cellulose paper and its application as surface flame retarded treatment for polypropylene. J Therm Anal Calorim. 2021;1:1–11.
11. Zhou K, Zhang Q, Liu J, Wang B, Jiang S, Shi Y, Hu Y, Gui Z. Synergetic effect of ferrocene and MoS_2 in polystyrene composites with enhanced thermal stability, flame retardant and smoke suppression properties. RSC Adv. 2014;4:13205–14.
12. Chen Y, Li J, Lai X, Li H, Zeng X. N-alkoxyamine-containing macromolecular intumescent flame-retardant-decorated zrp nanosheet and their synergism in flame-retarding polypropylene. Polym Adv. Technol. 2021; 1–13.
13. Nyambo C, Songtipya P, Manias E, Jimenez-Gasco MM, Wilkie CA. Effect of MgAl-layered double hydroxide exchanged with linear alkyl carboxylates on fire-retardancy of PMMA and PS. J Mater Chem. 2008;18:4827–38.
14. Huang SC, Deng C, Chen H, Li YM, Zhao ZY, Wang SX, Wang YZ. Novel ultrathin layered double hydroxide nanosheets with in situ formed oxidized phosphorus as anions for simultaneous fire resistance and mechanical enhancement of thermoplastic polyurethane. ACS Appl Polym Mater. 2019;1:1979–90.
15. Ning H, Ma Z, Zhang Z, Zhang D, Wang Y. Core-shell expandable graphite @ layered double hydroxide as a flame retardant for polyvinyl alcohol. J Therm Anal Calorim. 2021;7:1–10.
16. Attia NF, Saleh BK. Novel synthesis of renewable and green flame-retardant, antibacterial and reinforcement material for styrene–butadiene rubber nanocomposites. J Therm Anal Calorim. 2020;139:1817–27.
17. Wang X, Kalali EN, Wan JT, Wang DY. Carbon-family materials for flame retardant polymeric materials. Prog Polym Sci. 2017;69:22–46.
18. Attia NF, Sally EA, Elashery AM, Abdelazeem SE, Hyunchul O. Recent advances in graphene sheets as new generation of flame retardant materials. Mater Sci Eng B. 2021;274:115460.
19. Attia N F. Sustainable and efficient flame retardant materials for achieving high fire safety for polystyrene composites. J Therm Anal Calorim. 2021: 1–10.
20. Han Y, Wu Y, Shen M, Huang X, Zhu J, Zhang X. Preparation and properties of polystyrene nanocomposites with graphite oxide and graphene as flame retardants. J Mater Sci. 2013;48:4214–22.
21. Attia NF, Abd El-Aal NS, Hassan MA. Facile synthesis of graphene sheets decorated nanoparticles and flammability of their polymer nanocomposites. Polym Degrad Stab. 2016;126:65–74.
22. Xing W, Yang W, Yang W, Hu Q, Si J, Lu H, Yang B, Song L, Hu Y, Yuen RKK. Functionalized carbon nanotubes with phosphorus- and nitrogen-containing agents: effective reinforcer for thermal, mechanical, and flame-retardant properties of polystyrene nanocomposites. ACS Appl Mater Interfaces. 2016;8:26266–74.
23. Khose RV, Pethsangave DA, Wadekar PH, Ray AK, Some S. Novel approach towards the synthesis of carbon-based transparent highly effective flame retardant. Carbon. 2018;139:205–9.

24. Rahimi-Aghdam T, Shariatinia Z, Hakkarainen M, Haddadi-Asl V. Nitrogen and phosphorous doped graphene quantum dots: excellent flame retardants and smoke suppressants for polyacrylonitrile nanocomposites. J Hazard Mater. 2020;381:121013.
25. Ma R, Zeng M, Huang D, Wang J, Cheng Z, Wang Q. Amphiphilicity-adaptable graphene quantum dots to stabilize ph-responsive pickering emulsions at a very low concentration. J Colloid Interface Sci. 2021;601:106–13.
26. Yin G, Zheng Z, Wang H, Du Q, Zhang H. Preparation of graphene oxide coated polystyrene microspheres by pickering emulsion polymerization. J Colloid Interface Sci. 2013;394:192–8.
27. Liu Y, Zhang Y, Duan L, Zhang W, Su M, Sun Z, He P. Polystyrene/graphene oxide nanocomposites synthesized via pickering polymerization. Prog Org Coat. 2016;99:23–31.
28. Xu Q, Mensah RA, Jin C, Jiang L. A critical review of the methods and applications of microscale combustion calorimetry for material flammability assessment. J Therm Anal Calorim. 2021;7:1–13.
29. Jung R, Park WI, Kwon SM, Kim HS, Jin HJ. Location-selective incorporation of multiwalled carbon nanotubes in polycarbonate microspheres. Polymer. 2008;49:2071–6.
30. Maity N, Kuila A, Das S, Mandal D, Shit A, Nandi AK. Optoelectronic and photovoltaic properties of graphene quantum dot–polyaniline nanostructures. J Mater Chem A. 2015;3:20736–48.
31. Shi Y, Liu C, Liu L, Fu L, Yu B, Lv Y, Yang F, Song P. Strengthening, toughing and thermally stable ultra-thin MXene nanosheets/polypropylene nanocomposites via nanoconfinement. Chem Eng J. 2019;378:122267.
32. Lu H, Wilkie CA. Fire performance of flame retardant polypropylene and polystyrene composites screened with microscale combustion calorimetry. Polym Adv Technol. 2011;22:14–21.
33. Lu H, Wilkie CA, Ding M, Song L. Flammability performance of poly(vinyl alcohol) nanocomposites with zirconium phosphate and layered silicates. Polym Degrad Stab. 2011;96:1219–24.
34. Xu Q, Jin C, Majlingova A, Restas A. Discuss the heat release capacity of polymer derived from microscale combustion calorimeter. J Therm Anal Calorim. 2018;133:649–57.